

Progress towards a universal family of UV-IR extinction laws

**Jesús Maíz Apellániz¹, Emilio Trigueros Páez²,
Azalee Bostroem³, Rodolfo H. Barbá⁴,
and Christopher J. Evans⁵**

¹ **CAB, INTA-CSIC, Spain**

² **UCM, Spain**

³ **UCD, USA**

⁴ **ULS, Chile**

⁴ **ROE, UK**

Don't we know everything about the extinction laws already?

- Not really.
 - MIR: how do the water, aliphates, and silicates features vary among sightlines?
 - NIR: what is the slope of the power law? Is it universal?
 - Optical: what is the functional form? How do you include the diffuse interstellar bands (DIBs)? Can we find sightlines to measure the extinction law from 3000 \AA to $30 \mu\text{m}$ continuously?
 - Are the IR/optical and the UV extinction laws correlated or not?
 - Very few UV sightlines have been measured at low metallicity.
 - How does the extinction law vary with environment?
 - And more.
- All of the above affect a large number of astronomical measurements.

What are we doing about it?

- Already published.
 - A new family of optical/NIR extinction laws (Maíz Apellániz et al. 2014a) based on modern 30 Doradus data.
 - New UV sightlines in the SMC (Maíz Apellániz & Rubio 2012).
 - A preliminary analysis of the IR extinction (Maíz Apellániz 2015a).
 - The relationship between the optical DIBs and extinction (Maíz Apellániz et al. 2014b, Maíz Apellániz 2015b).
 - Studies of specific sightlines (Arias et al. 2006, Maíz Apellániz et al. 2015a, 2015b, 2015c).
 - Calibration (Maíz Apellániz 2004, 2005a, 2006, 2007, 2013a, 2013b).
- Work in progress (this poster).
 - Comparing different families of extinction laws in the Galaxy.
 - STIS 1700-10 200 Å spectrophotometry of 30 Doradus OB stars.
 - A study of the IR extinction with photometry and spectrophotometry.

Comparing extinction-law families

- Optical-NIR photometry for the GOSSS I+II+III sample (Sota et al. 2011, 2014, Maíz Apellániz et al. 2016). All have Johnson UBV and 2MASS JHK_s , some have Tycho-2 BV and/or Strömgren $uvby$.
- Fit the amount [$E(4405 - 5495)$] and type [R_{5495}] of extinction for each star using CHORIZOS (Maíz Apellániz 2004, 2013b) and three families of extinction laws: F99 (Fitzpatrick 1999), CCM (Cardelli et al. 1989) and M14 (Maíz Apellániz et al. 2014a). See Figure 1.
 - F99: poorest fits of all three families, especially for large values of R_{5495} .
 - CCM: overall better than F99 except for targets with Strömgren photometry due to its use of a seventh-degree polynomial in $1/\lambda$ for interpolation in the optical.
 - M14: best fits of all, with a reduced χ^2 always under 3.0.
- Even though the M14 family was derived using 30 Doradus data, it provides a better description of Galactic optical-NIR extinction than either the F99 or CCM families.

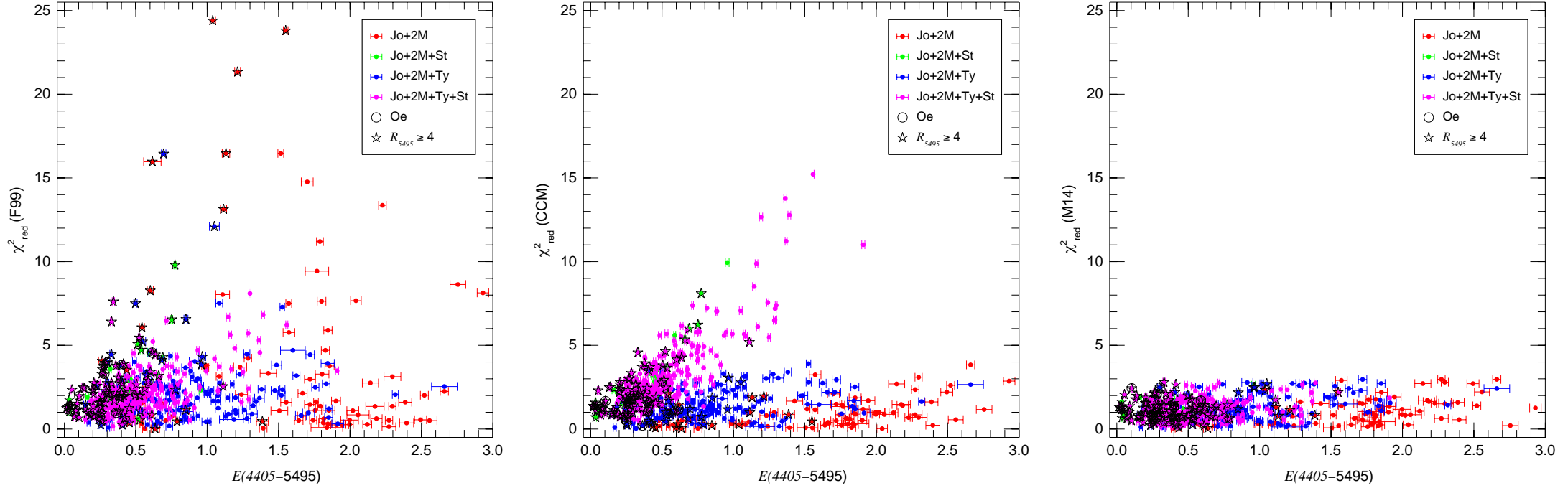


Figure 1. Reduced χ^2 of the CHORIZOS fit to the photometry of the GOSSS I+II+III sample as a function of the amount of extinction $E(4405 - 5495)$. The left, center, and right panels are for the F99, CCM, and M14 families of extinction laws, respectively. Different colors are used to indicate the photometric bands available for each star (Jo = Johnson UBV , 2M = 2MASS JHK_s , Ty = Tycho-2 BV , St = Strömgren $uvby$). Additional symbols are overplotted for Oe stars and objects with large values of R_{5495} (i.e. extinction caused by large grain sizes).

Amount and type of extinction

- We summarize the results of the M14 analysis in Figure 2.
- The majority of Galactic sightlines have R_{5495} between 3.0 and 3.5.
- At very low extinctions [$E(4405 - 5495) < 0.2$] the error bars on R_{5495} are too large to yield significant results.
- There are few stars with $R_{5495} < 3.0$ (sightlines with many small dust grains) but they are dominant among objects with large extinction.
- In the range $0.2 < E(4405 - 5495) < 1.2$ there is a significant fraction of stars with large values of R_{5495} . Those sightlines are depleted in small grains and are associated with H II regions.
- The R_{5495} histograms for the Galaxy and 30 Doradus are markedly different, with the latter showing a larger fraction of high- R_{5495} sightlines. The differences can be explained by [a] the lower values of $E(4405 - 5495)$ and [b] the larger fraction of H II region sightlines in 30 Doradus.

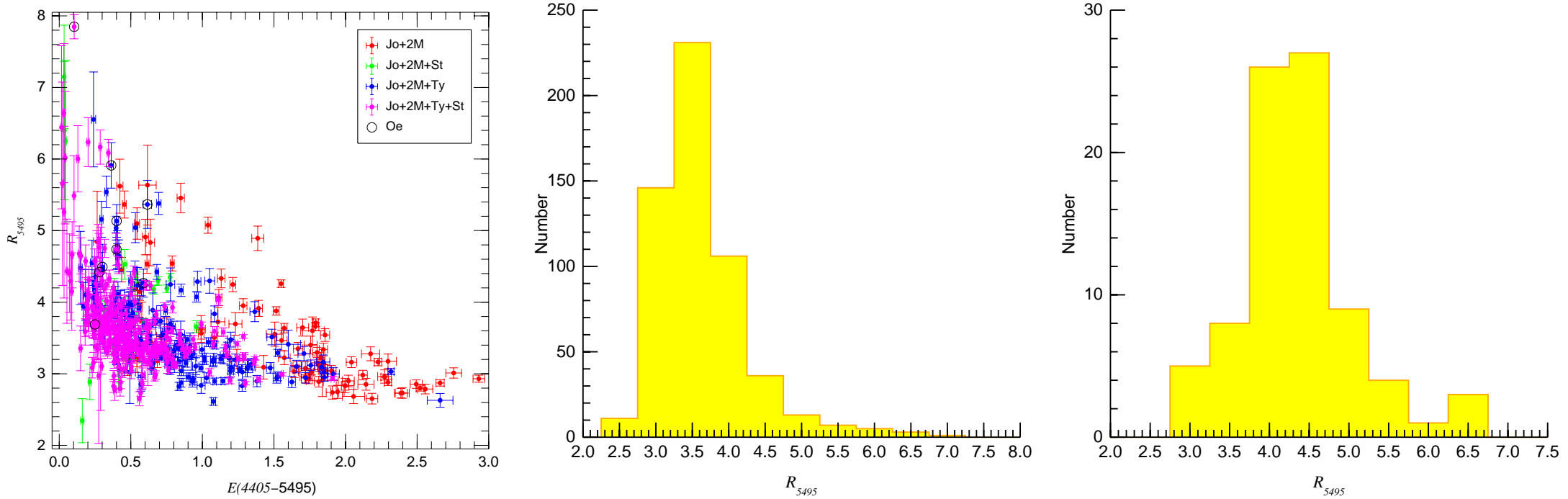


Figure 2. [left] R_{5495} as a function of $E(4405 - 5495)$ for the CHORIZOS fits for the GOSSS I+II+III sample using the M14 family of extinction laws. See Figure 1 for the symbol nomenclature. [center] R_{5495} histogram for the Galactic GOSSS I+II+III sample. [right] R_{5495} histogram for the 30 Doradus VFTS sample of Maíz Apellániz et al. (2014a).

30 Doradus with STIS

- HST cycle-23 STIS spectrophotometry program with 10 visits (7 executed, Figure 3).
- G230LB+G430L+G750L (1700-10 200 Å) with 2''-wide slit for 30 OB stars (Figures 4 and 5).
- Stellar spectra extracted with MULTISPEC (Maíz Apellániz 2005b) to eliminate nebular contamination.
- Different environments: H II region, diffuse ISM, molecular gas.
- Questions to answer:
 - What are the UV-NIR detailed (~ 100 Å resolution) extinction laws?
 - Is the Whitford (1958) knee real and does it exist for all values of R_{5495} ?
 - Are there real differences between the Galactic and 30 Doradus UV extinction laws?

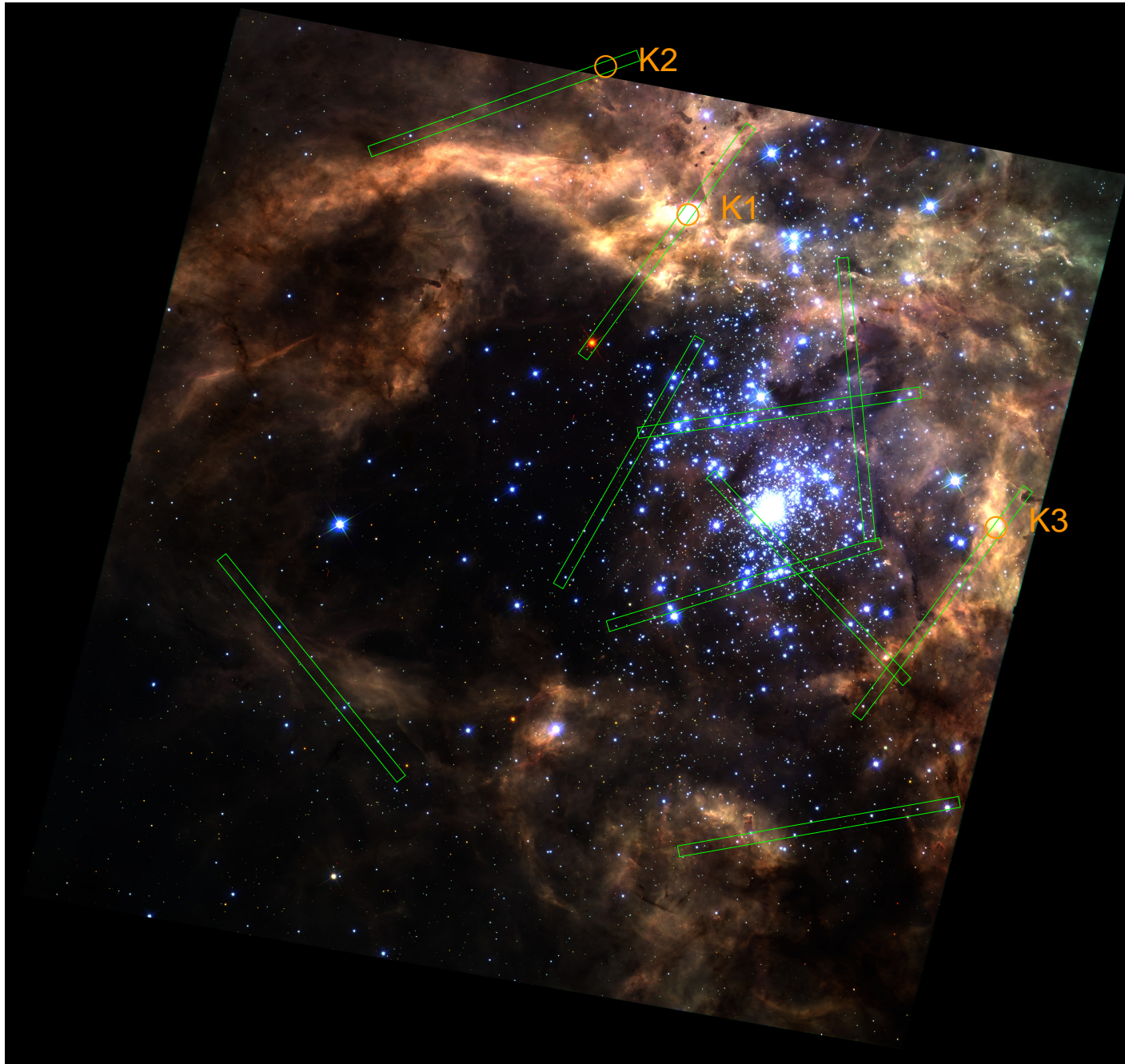


Figure 3. UVIS-WFC3 image of 30 Doradus with the ten STIS slits overlaid. The slit locations and PAs were selected to include a large variety of values of R_{5495} and of environments, from stellar cocoons to the diffuse ISM. Knots 1, 2, and 3 from Walborn et al. (2002) are marked. The field size is $206'' \times 194''$, N is top, and E is left.

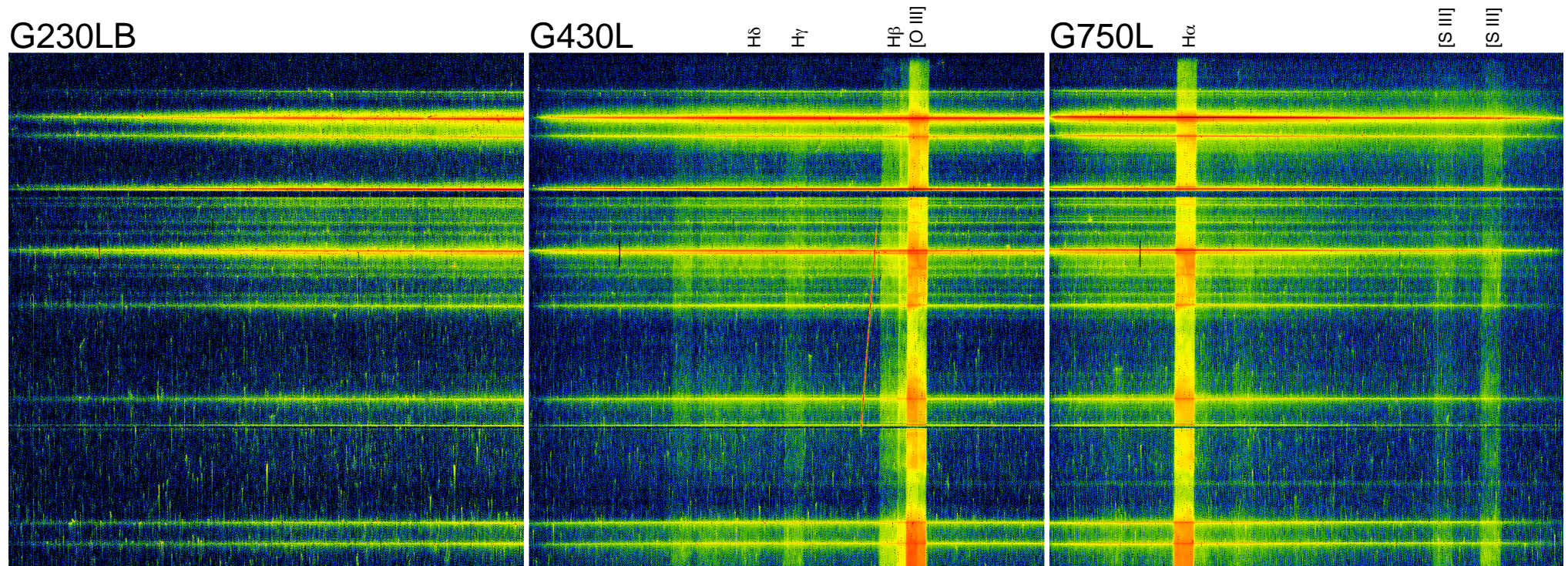


Figure 4. G230LB+G430L+G750L (1700-10 200 Å) STIS exposures of one of the ten 30 Doradus slits. The horizontal coordinate is wavelength and the vertical one is slit position (covering 51"). This slit covers a region close to R136 which is relatively dense in OB stars and has an intermediate nebular intensity. The positions of some prominent nebular lines are marked. Note that since we are using a 2"-wide slit, each nebular line creates a rectangular image in the CCD. The two horizontal dark regions are caused by occulting bars.

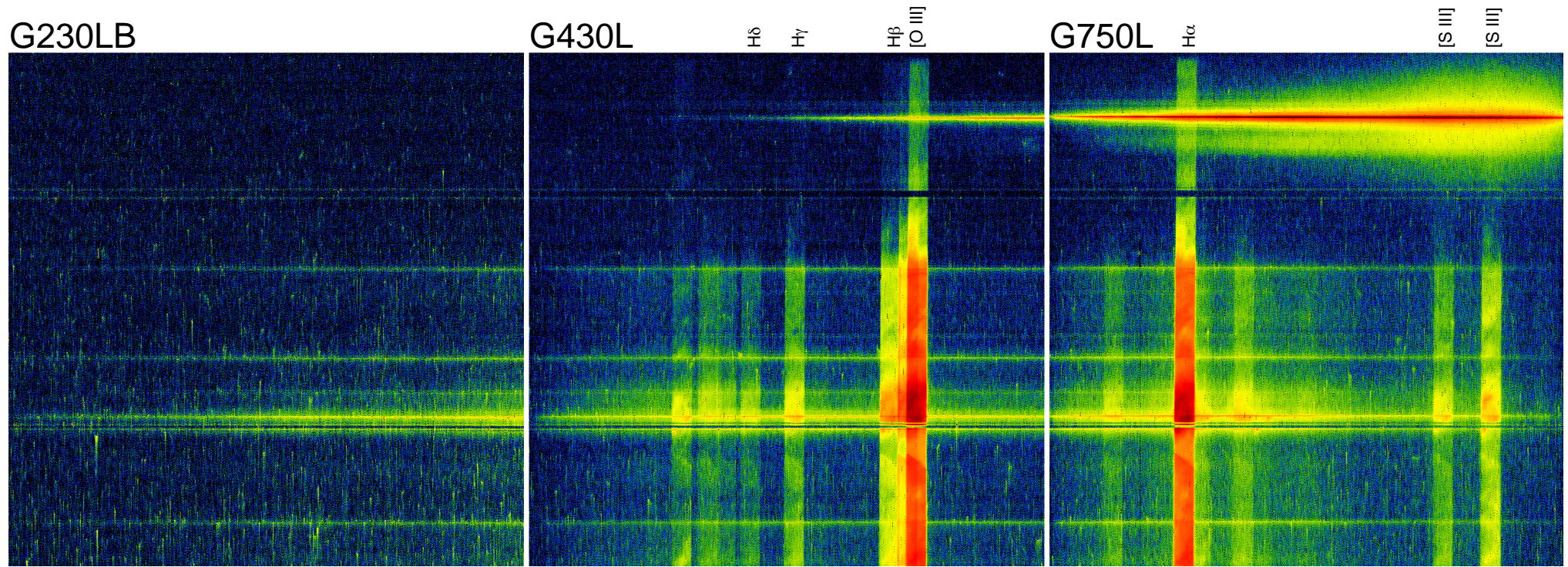


Figure 5. Same as Figure 4 but for a different slit. The lower half has several OB stars immersed in intense nebulosity while the upper half is dominated by a red supergiant in a region with little nebulosity.

Infrared extinction

- Objectives:
 - Derive a detailed IR extinction law for OB stars in the solar neighborhood.
 - Tie it up with the optical extinction law finding appropriate sightlines.
 - Analyze possible variations and relate them to R_{5495} .
- Methods:
 - Collect Spitzer+ISO spectrophotometry and Spitzer photometry for GOSSS stars.
 - Collect and reprocess WISE photometry.
 - Use WISE imaging to determine the type of environment.
 - Combine the data to fit: [a] atmosphere SED, [b] wind, and [c] extinction law for each sightline (Figure 6).

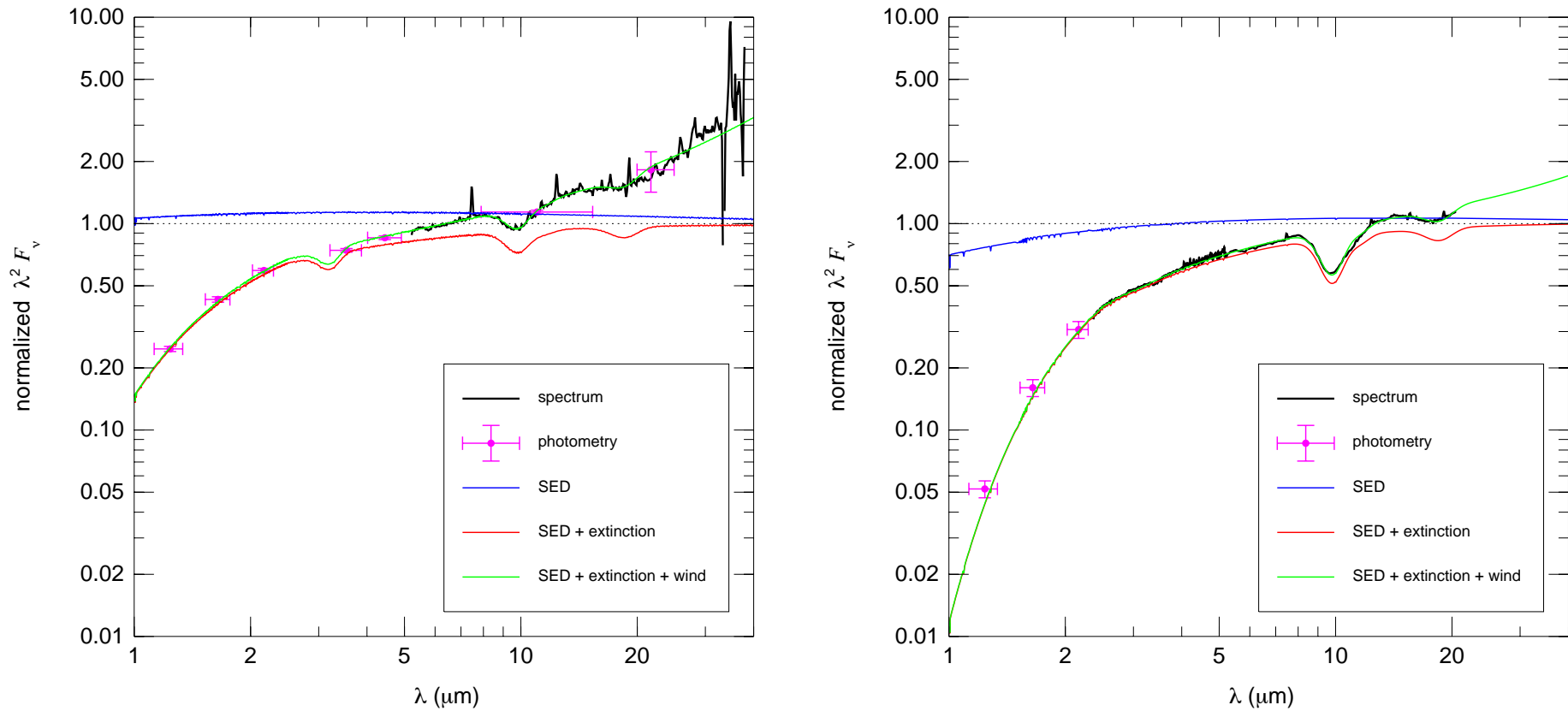


Figure 6. Two examples of atmosphere SED + wind + extinction law fits. [left] An O star with moderate extinction and strong wind with 2MASS JHK_s and WISE W1+W2+W3+W4 photometry and Spitzer spectrophotometry. [right] A B star with high extinction and moderate wind with 2MASS JHK_s photometry and ISO spectrophotometry. The vertical scale is $\lambda^2 F_\nu$ normalized to the atmosphere SED value at infinity.

WISE data

- MIR photometry for the GOSSS I+II+III sample.
 - Testing the validity of the W1+W2+W3+W4 photometry in the All-Sky (Cutri et al. 2012) and AllWISE (Cutri et al. 2013) releases.
 - Comparison of PSF photometry (data releases) and aperture photometry (new) using a realistic sky evaluation.
 - Saturation corrections and ID of cases with large uncertainties.
- Extinction and the environment.
 - WISE W3+W4 can be used to identify the presence of the warm dust associated with H II regions, detecting them even at high extinctions.
 - Morphological classification for the WISE images (Figure 7). Relationship to possible variations in the extinction law.
 - Main flag: I (isolated), n (weak nebulosity), N (strong nebulosity), S (saturated background i.e. bright H II region).
 - Optional flags: MO (hidden multiplicity in WISE, optical companion), MI (hidden multiplicity in WISE, IR companion), B (bow shock visible).

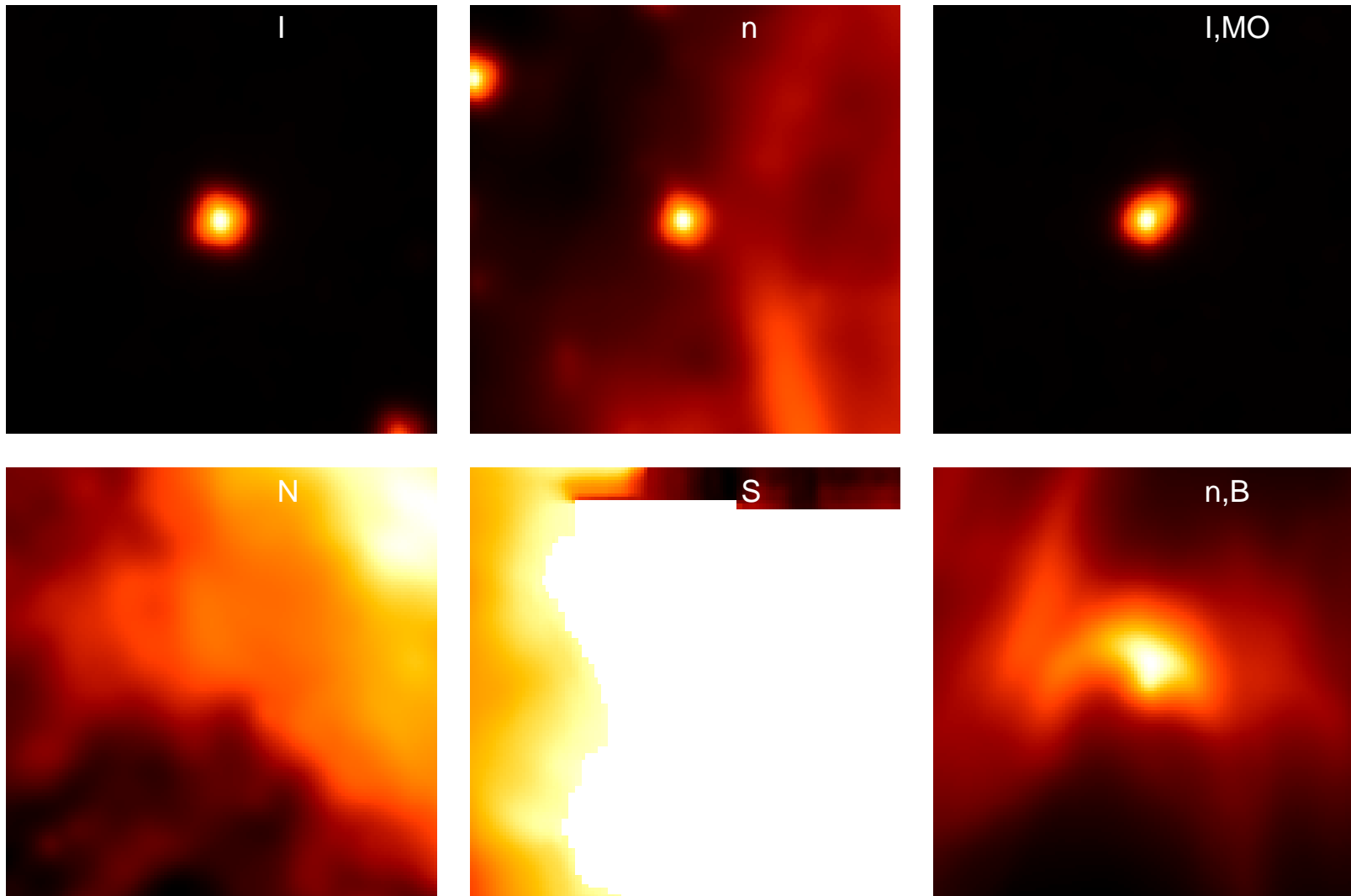


Figure 7. WISE W3 images and morphological classifications for six GOSSS I+II+III stars. Each field is $3' \times 3'$, with N towards the top and E towards the left, the target at the center, and a logarithmic intensity scale.

References

- Arias, J. I. et al. 2006, *MNRAS* **366**, 739.
- Cardelli, J. A. et al. 1989, *ApJ* **345**, 245.
- Cutri, R. M. et al. 2012, *VizieR Online Catalog II/311*.
- Cutri, R. M. et al. 2013, *VizieR Online Catalog II/328*.
- Fitzpatrick, E. L. 1999, *PASP* **111**, 63.
- Maíz Apellániz, J. 2004, *PASP* **116**, 859.
- Maíz Apellániz, J. 2005a, *PASP* **117**, 615.
- Maíz Apellániz, J. 2005b, *STIS-ISR 2005-02*.
- Maíz Apellániz, J. 2006, *AJ* **131**, 1184.
- Maíz Apellániz, J. 2007, *ASPC* **364**, 227.
- Maíz Apellániz, J. & Rubio, M. 2012, *A&A* **541**, 54.
- Maíz Apellániz, J. 2013a,
Highlights of Spanish Astrophysics VII, 583.
- Maíz Apellániz, J. 2013b,
Highlights of Spanish Astrophysics VII, 657.
- Maíz Apellániz, J. et al. 2014a, *A&A* **564**, 63.
- Maíz Apellániz, J. et al. 2014b, *IAUS* **297**, 117.
- Maíz Apellániz, J. 2015a,
Highlights of Spanish Astrophysics VIII, 402.
- Maíz Apellániz, J. 2015b, *MmSAI* **86**, 553.
- Maíz Apellániz, J. et al. 2015a, *A&A* **579**, 108.
- Maíz Apellániz, J. et al. 2015b, *A&A* **583**, 132.
- Maíz Apellániz, J. et al. 2015c,
Highlights of Spanish Astrophysics VIII, 604.
- Maíz Apellániz, J. et al. 2016, *ApJS* **224**, 4.
- Sota, A. et al. 2011, *ApJS* **193**, 24.
- Sota, A. et al. 2014, *ApJS* **211**, 10.
- Walborn, N. R. et al. 2002, *AJ* **124**, 1601.
- Whitford, A. E. 1958, *AJ* **63**, 201.